The Annals of Applied Statistics
2011, Vol. 5, No. 1, 551–577
DOI: 10.1214/10-AOAS376

A DYNAMIC BAYESIAN NONLINEAR MIXED-EFFECTS MODEL OF HIV RESPONSE INCORPORATING MEDICATION ADHERENCE, DRUG RESISTANCE AND COVARIATES[1]

BY YANGXIN HUANG, HULIN WU, JEANNE HOLDEN-WILTSE AND EDWARD P. ACOSTA

University of South Florida, University of Rochester, University of Rochester and University of Alabama

HIV dynamic studies have contributed significantly to the understanding of HIV pathogenesis and antiviral treatment strategies for AIDS patients. Establishing the relationship of virologic responses with clinical factors and covariates during long-term antiretroviral (ARV) therapy is important to the development of effective treatments. Medication adherence is an important predictor of the effectiveness of ARV treatment, but an appropriate determinant of adherence rate based on medication event monitoring system (MEMS) data is critical to predict virologic outcomes. The primary objective of this paper is to investigate the effects of a number of summary determinants of MEMS adherence rates on virologic response measured repeatedly over time in HIV-infected patients. We developed a mechanism-based differential equation model with consideration of drug adherence, interacted by virus susceptibility to drug and baseline characteristics, to characterize the long-term virologic responses after initiation of therapy. This model fully integrates viral load, MEMS adherence, drug resistance and baseline covariates into the data analysis. In this study we employed the proposed model and associated Bayesian nonlinear mixed-effects modeling approach to assess how to efficiently use the MEMS adherence data for prediction of virologic response, and to evaluate the predicting power of each summary metric of the MEMS adherence rates. In particular, we intend to address the questions: (i) how to summarize the MEMS adherence data for efficient prediction of virologic response after accounting for potential confounding factors such as drug resistance and covariates, and (ii) how to evaluate treatment effect of baseline characteristics interacted with adherence and other clinical factors. The approach is applied to an AIDS clinical trial involving 31 patients who had available data as required for the proposed model. Results demonstrate that the appropriate determinants of MEMS adherence rates are important in order to more efficiently predict virologic response, and investigations of adherence to ARV treatment would benefit from measuring not only adherence rate but also its summary metric assessment. Our study also shows that the mechanism-based dynamic model is powerful and effective to establish a relationship of virologic responses with medication adherence, virus resistance to drug and baseline covariates.

Received May 2009; revised September 2009.

[1]Supported in part by NIAID/NIH Grant AI080338 and MSP/NSA Grant H98230-09-1-0053 to Y. Huang, and NIH Grants AI50020, AI078498, AI078842 and AI087135 to H. Wu.

Key words and phrases. Bayesian mixed-effects models, confounding factors, HIV dynamics, longitudinal data, MEMS adherence assessment, time-varying drug efficacy, virus resistance.

1. Introduction. The revolution in human immunodeficiency virus (HIV) treatment has brought diagnostic tests that can accurately measure levels of HIV in blood. Resulting data show (plasma) viral load (HIV-1 RNA copies or RNA copies) to be an important predictor of the risk of progression to AIDS. The antiretroviral (ARV) agents, which include potent protease inhibitors (PIs) are, however, not a cure for HIV infection. While many patients benefit from ARV treatment, others do not benefit or only experience a temporary benefit. There are several reasons why treatment fails, of which poor patient adherence to ARV therapy is a leading factor [Ickovics and Meisler (1997); Paterson et al. (2000)]. Thus, assessment of adherence within AIDS clinical trials is a critical component of the successful evaluation of therapy outcomes. Maintaining adherence may be particularly difficult when the drug regimen is complex or side-effects are severe, as is often the case for current HIV therapy [Ickovics and Meisler (1997)].

The measurement of adherence remains problematic; a standard definition of adherence and completely reliable measures of adherence are lacking. Nevertheless, there has been substantial progress in both of these areas in the past few years. First, it appears that higher levels of adherence are needed for HIV disease than other diseases to achieve the desired therapeutic benefit [Paterson et al. (2000)]. Second, better appreciation of the value and limitations of different adherence measurements has been addressed [Bova et al. (2005)]. In AIDS clinical trials adherence to medication regimen is currently measured by two methods: by use of questionnaires (patient self-reporting and/or face-to-face interview) and by use of electronic compliance monitoring (Medication Event Monitoring System [MEMS]) caps. The MEMS is often used as an objective adherence measure. It consists of a computer chip in the cap of a medication bottle that records each time the bottle is opened. The results can be downloaded, printed out and analyzed. It demonstrates that medication-taking patterns are highly variable among patients [Kastrissios et al. (1998)] and that they often give a more precise measure of adherence than self-report [Arnsten et al. (2001)]. However, MEMS data are also subject to error and are not widely available in the clinical setting. Adherence assessment by self-report is usually evaluated by a patient's ability to recall their medication dosing during a specific time interval. Finally, it is important to note that the measurement of viral load levels is of special utility as an indirect measure of adherence in HIV therapeutics. It has been argued that this is not an adherence measure because other factors may influence viral load (drug resistance, etc.). However, there is a tight correlation between viral load and adherence [Paterson et al. (2000); Haubrich et al. (1999)].

Viral dynamic models can be formulated through ordinary differential equations (ODE), but there has been only limited development of statistical methodologies for assessing their agreement with observed data. Currently there also are substantial knowledge gaps between theoretical HIV dynamics and the role of many clinical factors. In developing long-term dynamic modeling, this paper will address these problems by utilizing time-specific information, such as drug adherence and susceptibility factors, on the biological mechanism of HIV dynamics to

achieve more realistic and accurate characterization of the relationship between clinical/drug factors and virologic response. Several studies [Arnsten et al. (2001); Levine et al. (2006)] investigated the association between virologic responses and adherence assessed by both questionnaire and MEMS data. The results indicated that the MEMS cap adherence data may not be correlated better to virologic response compared to the questionnaire adherence data unless the MEMS cap data are summarized in an appropriate way. Further, Huang et al. (2008), Labbé and Verotta (2006), Liu et al. (2007) and Vrijens et al. (2005) modeled the relationship between virologic response and adherence rate using questionnaire data and MEMS data averaged by each interval between study visits or weekly basis, but no significant differences were found in predicting virologic response. Along with this line, this paper will investigate different determinants of the adherence rate based on MEMS data from an AIDS clinical trial study [Hammer et al. (2002)] and compare their performance for predicting a virological response. We employed the proposed mechanism-based dynamic model to assess how to efficiently use the adherence data based on MEMS to predict virological response. In particular, we intend to address the questions (i) how to summarize the MEMS adherence data for efficient prediction of virological response after accounting for potential confounding factors such as drug resistance and baseline covariates, and (ii) how to evaluate treatment effect of baseline characteristics interacted with MEMS adherence and other clinical factors.

The purpose of this paper is to describe a reparameterized ODE dynamic model (with identifiable parameters) which fully integrates viral load, medication adherence, drug resistance and baseline covariates data from an AIDS clinical trial study into the analysis. Thus, our dynamic model will be able to characterize sustained suppression or resurgence of the virus as arising from intrinsic viral dynamics, and/or influenced by factors such as drug susceptibility and adherence during the treatment period of the clinical trial. The Bayesian nonlinear mixed-effects (BNLME) modeling approach [Davidian and Giltinan (1995)] is employed to estimate dynamic parameters and identify significant clinical factors and/or covariates on virologic response to ARV treatment. The rest of this article is organized as follows. Section 2 introduces reparameterized viral dynamic models with time-varying drug efficacy which incorporates the effects of drug adherence, drug resistance and baseline covariates, and briefly describes the BNLME modeling approach, implemented via Markov chain Monte Carlo (MCMC) procedures, followed by defining the deviance information criterion (DIC) for comparison of models. In Section 3 we summarize the motivating data set from an AIDS clinical trial study including the data of plasma viral load, medication adherence from MEMS cap, drug resistance and baseline covariates; the proposed methodology is applied to these data and the results are presented. The method is evaluated via a simulation study in Section 4. Finally, we conclude the article with some discussions in Section 5.

2. HIV dynamic mechanism-based ODE models and statistical approaches. This section aims to introduce long-term viral dynamic models based on a system of ODE with time-varying coefficients but without closed-form solutions, and to investigate associated methodologies to demonstrate the application of these models to an AIDS clinical trial study. Long-term viral dynamic models can be used to describe the interaction between cells susceptible to target cells (T), infected cells (T^*) and free virus (V) by considering time-varying drug efficacy [Huang and Wu (2006); Huang et al. (2006)]. These three compartments (variables) are described as follows.

HIV virions (V) will infect target cells (T) and turn them into infected cells (T^*) at an infection rate k. Due to the intervention of antiviral drugs, we assume that drugs reduce the infection rate in the infected cells (T^*) by $1-\gamma(t)$ $[0 \le \gamma(t) \le 1]$. The infected cells will die at rate δ after producing an average of N virions per cell during their lifetimes, and free virions are removed from the system at rate c. In addition to the dynamics describing virus infection, we have to specify the dynamics of the uninfected cell population. The simplest assumption is that uninfected cells are produced at a constant rate λ at which new T cells are generated from sources within the body, such as the thymus and die at a rate d_T. Thus, the HIV dynamic model, after initiation of antiviral therapy, can be written as

$$
\begin{aligned}
\frac{d}{dt}T(t) &= \lambda - d_T T(t) - [1-\gamma(t)]kT(t)V(t),\\
\frac{d}{dt}T^*(t) &= [1-\gamma(t)]kT(t)V(t) - \delta T^*(t),\\
\frac{d}{dt}V(t) &= N\delta T^*(t) - cV(t),
\end{aligned}
\tag{1}
$$

where the time-varying parameter $\gamma(t)$ (as defined below) quantifies the time-varying drug efficacy. If the regimen is not 100% effective [i.e., $0 \le \gamma(t) < 1$], the system of ODE cannot be solved analytically. The solutions to (1) then have to be evaluated numerically. When $\gamma(t) = \gamma_0$ (an unknown constant), the model (1) becomes the model developed by Perelson and Nelson (1999). In particular, when $\gamma(t) = 0$ (the drug has no effect), the model (1) reduces to the model in the publications [Bonhoeffer et al. (1997); Nowak et al. (1995, 1997, 2000); Stafford et al. (2000)]; while $\gamma(t) = 1$ (the drug is 100% effective), the model (1) reverts to the model discussed by Nowak and May (2000) and Perelson and Nelson (1999).

However, it is challenging to estimate all the parameters in the model (1) and to conduct inference because the model (1) is not a priori identifiable (i.e., multiple sets of parameters obtain identical fits to the data), given only viral load measurements [Cobelli et al. (1979)]. To obtain a model with a priori identifiable parameters [Labbé and Verttoa (2006)], this paper investigates mechanism-based reparameterized ODE models to quantify the long-term viral dynamics with ARV treatment and the associated statistical methods for model fitting.

2.1. *Reparameterized model with time-varying drug efficacy.* Following the studies [Perelson and Nelson (1999); Nowak and May (2000); Labbé and Verttoa (2006)], we reparameterize the model (1) using the rescaled variables $\widetilde{T}(t) = (d_T/\lambda)T(t)$, $\widetilde{T}^*(t) = (\delta/\lambda)T^*(t)$, $\widetilde{V}(t) = (k/d_T)V(t)$. These yield the rescaled version as follows:

$$
\begin{aligned}
\frac{d}{dt}\widetilde{T}(t) &= \frac{d_T}{\lambda}\frac{d}{dt}T = d_T\{1 - \widetilde{T}(t) - [1-\gamma(t)]\widetilde{T}(t)\widetilde{V}(t)\},\\
\frac{d}{dt}\widetilde{T}^*(t) &= \frac{\delta}{\lambda}\frac{d}{dt}T^*(t) = \delta\{[1-\gamma(t)]\widetilde{T}(t)\widetilde{V}(t) - \widetilde{T}^*(t)\},\\
\frac{d}{dt}\widetilde{V}(t) &= \frac{k}{d_T}\frac{d}{dt}V(t) = c\{R\widetilde{T}^*(t) - \widetilde{V}(t)\},
\end{aligned}
\tag{2}
$$

where $R = kN\lambda/(cd_T)$ represents the basic reproductive ratio for the virus, defined as the number of newly infected cells that arise from any one infected cell when almost all cells are uninfected [Nowak and May (2000)]. Note that the rescaled model (2) has fewer parameters than the 'original' model (1). The identifiability of the model (2) is guaranteed [Cobelli et al. (1979); Labbé and Verttoa (2006)] and parameters of the model can be uniquely identified. If $R < 1$, then the virus will not spread, since every infected cell will on average produce less than one infected cell. If, on the other hand, $R > 1$, then every infected cell will on average produce more than one newly infected cell and the virus will proliferate. For the HIV virus to persist in the host, infected cells must produce at least one secondary infection, and R must be greater than unity [Nowak and May (2000)].

Assuming steady state before the beginning of drug therapy, initial conditions for the model can now be expressed as simple functions of the initial conditions for viral load ($\widetilde{V}_0$): $\widetilde{T}_0 = 1/(1+\widetilde{V}_0)$, $\widetilde{T}_0^* = \widetilde{V}_0/(1+\widetilde{V}_0)$, $\widetilde{V}_0 = \widetilde{V}(0)$ [Cobelli et al. (1979); Labbé and Verttoa (2006)]. The assumption of initial steady state is necessary to guarantee identifiable (none of the models reported or referenced here is identifiable if the initial states are unknown), and is often justified by the clinical trial protocol. For example, in ACTG 398, individual patients were taken off the drug before the initiation of the new therapy (washout period to eliminate the effect of previously administered drugs and to guarantee that all individuals started from steady-state conditions). Finally, viral load $[V(t)]$ in model (1) is related to an equation output of viral load amount $[\widetilde{V}(t)]$ in model (2) as follows: $V(t) = \rho\widetilde{V}(t)$, where ρ, which is equivalent to a volume of distribution of pharmacokinetics, is a viral load scaling (proportionality) factor (10,000 copies/ml) to be estimated from the data [Nowak and May (2000)]. The set of ODE (2) will be used to construct the BNLME model.

2.2. *Time-varying drug efficacy model.* Within the population of HIV virions in a human host, there is likely to be genetic diversity and corresponding diversity in susceptibility to the various ARV agents. In clinical practice, genotypic or

phenotypic tests can be performed to determine the sensitivity of HIV-1 RNA to ARV agents before a treatment regimen is selected. Here we use the phenotypic marker, IC_{50} [Molla et al. (1996)], to quantify agent-specific drug susceptibility. Because experimental data tracking development of resistance suggest that the resistant fraction of the viral population grows exponentially, we propose a model of log-linear function to approximate the within-host changes over time in IC_{50} as follows:

$$IC_{50}(t) = \begin{cases} \log\left(S_0 + \dfrac{S_f - S_0}{t_f} t\right) & \text{for } 0 < t < t_f, \\ \log(S_f) & \text{for } t \geq t_f, \end{cases}$$

where S_0 and S_f are respective values of $IC_{50}(t)$ at baseline and time point t_f at which the resistant mutations dominate. In our study, t_f is the time of virologic failure which is observed from clinical studies. If $S_f = S_0$, no new drug resistant mutation is developed during treatment. Although more complicated models for median inhibitory concentration have been proposed based on the frequencies of resistant mutations and cross-resistance patterns [Wainberg et al. (1996); Bonhoeffer, Lipsitch and Levin (1997)], in clinical studies or clinical practice it is common to collect IC_{50} values only at baseline and failure time as designed in ACTG 5055 [Acosta et al. (2004)] and ACTG 398 [Hammer et al. (2002); Pfister et al. (2003)]. Thus, given that IC_{50} is only measured at baseline and at the time of treatment failure, this function may serve as a good approximation in terms of data availability.

Poor adherence to a treatment regimen is one of the major causes of treatment failure [Ickovics and Meisler (1997)]. The following model is used to represent adherence for a time interval $T_k < t \leq T_{k+1}$:

$$A(t) = \begin{cases} 1, & \text{if all doses are taken in } (T_k, T_{k+1}], \\ r_k, & \text{if } 100r_k\% \text{ doses are taken in } (T_k, T_{k+1}], \end{cases}$$

where $0 \leq r_k < 1$, with r_k indicating the adherence rate computed for each assessment interval $(T_k, T_{k+1}]$ between study visits based on the questionnaire or MEMS data; T_k denotes the kth adherence assessment time.

In most viral dynamic studies, investigators assumed that either drug efficacy was constant over treatment time [Perelson and Nelson (1999); Wu and Ding (1999)] or antiviral regimens had perfect effect in blocking viral replication [Ho et al. (1995); Perelson et al. (1996)]. However, the drug efficacy may change as concentrations of ARV drugs and other factors (e.g., drug resistance) vary during treatment. A simple pharmacodynamic sigmoidal $E_{\max}$ model for dose–effect relationship is [Gabrielsson and Weiner (2000)]

$$E = \frac{E_{\max} C}{EC_{50} + C}, \tag{3}$$

where $E_{\max}$ is the maximal effect that can be achieved, C is the drug concentration, and EC_{50} is the drug concentration that induced an effect equivalent to 50%

of the maximal effect. Many different variations of the $E_{\max}$ model have been developed by pharmacologists to model pharmacodynamic effects. $E_{\max}$ models include the sigmoid $E_{\max}$ model, the ordinary $E_{\max}$ model and composite $E_{\max}$ models [Gabrielsson and Weiner (2000); Davidian and Giltinan (1995)]. The ordinary $E_{\max}$ model describes agonistic and antagonistic (inhibitory) effects of a drug, the sigmoid $E_{\max}$ model is more flexible for the steepness or curvature of the response–concentration curve compared to the ordinary $E_{\max}$ model, and composite $E_{\max}$ models are used for multiple drug effects. More detailed discussions on $E_{\max}$ models can be found in the book by Gabrielsson and Weiner (2000) and the paper by Huang et al. (2003). Here we employ the following modified $E_{\max}$ model to represent the time-varying drug efficacy for two ARV agents within a class,

$$\gamma(t) = \frac{A_1(t)/IC_{50}^1(t) + A_2(t)/IC_{50}^2(t)}{\phi + A_1(t)/IC_{50}^1(t) + A_2(t)/IC_{50}^2(t)}, \tag{4}$$

where $A_k(t)$ and $IC_{50}^k(t)$ $(k = 1, 2)$ are the adherence profile of the drug as measured by MEMS data and the time-course of median inhibitory concentrations for the two drugs, respectively; $\phi = \exp(\beta_0 + \beta_1 w_1 + \beta_2 w_2)$; w_1 and w_2 are observed baseline viral load and CD4 cell count, respectively; $\boldsymbol{\beta} = (\beta_0, \beta_1, \beta_2)^T$ are unknown covariate effect parameters to be estimated from clinical data. If $\beta_1 = \beta_2 = 0$ (without considering effect of covariates), $\phi = \exp(\beta_0)$ can be used to quantify the conversion between in vitro and in vivo IC_{50} which is the case discussed by Huang et al. (2003). If $\gamma(t) = 1$, the drug is 100% effective, whereas if $\gamma(t) = 0$, the drug has no effect. Note that, if $A_k(t)$, $IC_{50}^k(t)$, w_1 and w_2 are measured or obtained from a clinical study and $\boldsymbol{\beta}$ can be estimated from clinical data, then the time-varying drug efficacy $\gamma(t)$ can be estimated for the whole period of ARV treatment.

2.3. *Bayesian modeling approaches*. A number of studies investigated various statistical methods, including Bayesian approaches, to fit viral dynamic models and to predict virological responses [Han et al. (2002); Huang et al. (2006); Perelson et al. (1996); Wu et al. (1998); Wu and Ding (1999)]. The Bayesian approach to viral dynamic modeling is particularly appealing from a biological perspective, as it allows informative prior distributions to be incorporated. From a statistical estimation point of view, a Bayesian approach is preferable because of the difficulties which are often encountered from a classical approach when models involve the large numbers of parameters, and complex nonlinearity of the subject-specific models. A Bayesian nonlinear mixed-effects (BNLME) model allows us to incorporate prior information at the population level into the estimates of dynamic parameters for individual subjects. We briefly summarize the main concepts in the Bayesian approach to inference and the presentation is, of course, far from exhaustive [Davidian and Giltinan (1995); Gelfand and Smith (1990); Huang et al. (2006); Wakefield et al. (1994); Wakefield (1996)].

In reference to the model (2), we denote the number of subjects by n and the number of measurements on the ith subject by m_i. Let $\boldsymbol{\mu} = (\log c, \log \delta, \log d_T, \log \rho, \log R, \beta_0, \beta_1, \beta_2)^T$, $\boldsymbol{\Theta} = \{\boldsymbol{\theta}_i, i = 1, \ldots, n\}$, $\boldsymbol{\theta}_i = (\log c_i, \log \delta_i, \log d_{Ti}, \log \rho_i, \log R_i, \log \phi_i)^T$ and $\mathbf{Y} = \{y_{ij}, i = 1, \ldots, n; j = 1, \ldots, m_i\}$. Let $f_{ij}(\boldsymbol{\theta}_i, t_j) = \log_{10}(V(\boldsymbol{\theta}_i, t_j))$, where $V(\boldsymbol{\theta}_i, t_j)$ is proportional to the numerical solution of $\widetilde{V}(t)$ in the differential equations (2) for the ith subject at time t_j. Let $y_{ij}(t)$ and $e_i(t_j)$ denote the repeated measurements of viral load in $\log_{10}$ scale and a measurement error with mean zero, respectively. Note that log-transformation of dynamic parameters and viral load is used to make sure that estimates of dynamic parameters are positive and to stabilize the variance and convergence, respectively. The BNLME model can be written in the following three levels [Gelfand and Smith (1990); Davidian and Giltinan (1995); Huang and Wu (2006); Wakefield (1996)].

Level 1. Within-subject variation:

$$\mathbf{y}_i = \mathbf{f}_i(\boldsymbol{\theta}_i) + \mathbf{e}_i, \qquad \mathbf{e}_i|\sigma^2, \boldsymbol{\theta}_i \sim \mathcal{N}(\mathbf{0}, \sigma^2 \mathbf{I}_{m_i}), \tag{5}$$

where $\mathbf{y}_i = (y_{i1}(t_1), \ldots, y_{im_i}(t_{m_i}))^T$, $\mathbf{f}_i(\boldsymbol{\theta}_i) = (f_{i1}(\boldsymbol{\theta}_i, t_1), \ldots, f_{im_i}(\boldsymbol{\theta}_i, t_{m_i}))^T$, $\mathbf{e}_i = (e_i(t_1), \ldots, e_i(t_{m_i}))^T$.

Level 2. Between-subject variation:

$$\boldsymbol{\theta}_i = \mathbf{W}_i \boldsymbol{\mu} + \mathbf{b}_i, \qquad [\mathbf{b}_i|\boldsymbol{\Sigma}] \sim \mathcal{N}(\mathbf{0}, \boldsymbol{\Sigma}), \tag{6}$$

where $\mathbf{b}_i$ are random effects with mean zero. It is noteworthy that, for $\boldsymbol{\beta} = (\beta_0, \beta_1, \beta_2)^T$, no log-transformation is required as they are not necessarily positive. $\mathbf{W}_i = (\mathbf{I}_6, \mathbf{J}_{1i}, \mathbf{J}_{2i})$, where $\mathbf{I}_6$ is an identity matrix and $\mathbf{J}_{si} = (0, 0, 0, 0, 0, w_{si})^T$ $(s = 1, 2; i = 1, 2, \ldots, n)$ are 6×1 vector, with w_{1i} and w_{2i} being (standardized) individual baseline viral load (in $\log_{10}$ scale) and CD4 cell count, respectively. For $\boldsymbol{\beta} = (\beta_0, \beta_1, \beta_2)^T$, we are only interested in estimating them at population level. Thus, the individual parameter ϕ_i is related to them as follows, $\log \phi_i = \beta_0 + \beta_1 w_{1i} + \beta_2 w_{2i} + b_{i6}$, where b_{i6} is the last element of $\mathbf{b}_i$ $(i = 1, 2, \ldots, n)$.

Level 3. Hyperprior distributions:

$$\sigma^{-2} \sim Ga(a, b), \qquad \boldsymbol{\mu} \sim \mathcal{N}(\boldsymbol{\eta}, \boldsymbol{\Lambda}), \qquad \boldsymbol{\Sigma}^{-1} \sim Wi(\boldsymbol{\Omega}, \nu), \tag{7}$$

where the mutually independent Gamma (Ga), Normal ($\mathcal{N}$) and Wishart (Wi) prior distributions are chosen to facilitate computations [Davidian and Giltinan (1995)]. The hyper-parameters a, b, $\boldsymbol{\eta}$, $\boldsymbol{\Lambda}$, $\boldsymbol{\Omega}$ and ν can be determined from previous studies and literature.

The Bayesian approach is developed in the presence of observations whose value is initially uncertain and described through a probability distribution, which depends on some parameters. In the applications we assume that the researcher has some knowledge about at least some of the parameters which often represent characteristics of interest describing the process. The Bayesian approach incorporates this information through prior distribution into observed data to obtain

its posterior distribution. While computation of the posterior distribution involves solving multidimensional integrals, the introduction of Markov chain Monte Carlo (MCMC) methods such as the Gibbs sampler and Metropolis–Hastings algorithm opened the way to analysis of complex models through decomposition and sampling from full conditional distributions; see Gamerman (1997) and Gilks et al. (1995) for general theory and implementation details. Some more specific discussion of the Bayesian dynamic modeling approach, including the choice of the hyper-parameters, the iterative MCMC algorithm and the implementation of the MCMC procedures can be found in publications by Huang and Wu (2006) and Wakefield (1996). The Bayesian approach was developed and tailored as required by the unique features of the proposed HIV dynamic models. The basic principles of these proposed methodologies were well established in the statistical literature [Gamerman (1997); Gilks et al. (1995); Wakefield (1996)], but the applications of these methods in this paper are nonetheless innovative within the context of a system of nonlinear ODE of time-varying coefficient, but without a closed-form solution.

The progress in Bayesian posterior computation due to MCMC procedures has made it possible to fit increasingly complex statistical models [Huang and Wu (2006); Wakefield (1996)] and entailed the wish to determine the best fitting model in a class of candidates. Thus, it has become more and more important to develop efficient model selection criteria. A recent publication by Spiegelhalter et al. (2002) suggested a generalization of the Akaike information criterion (AIC) [Akaike (1973)] and related also to the Bayesian information criterion (BIC) [Schwarz (1978)] that is deviance information criterion (DIC). In this paper we demonstrate its usefulness to compare BNLME models for longitudinal HIV dynamics discussed previously. For completeness, a brief summary of DIC follows. More detailed discussion of DIC and its properties can be found in publications by Spiegelhalter et al. (2002) and Zhu and Carlin (2000).

Assume that the distribution of the data, $\mathbf{Y}$, depends on the parameter vector $\boldsymbol{\Psi}$. Most recently, Spiegelhalter et al. (2002) suggested examining the posterior distribution of the deviance statistics defined by

$$D(\boldsymbol{\Psi}) = -2\log p(\mathbf{Y}|\boldsymbol{\Psi}) + 2\log g(\mathbf{Y})$$

for Bayesian model comparison, where $p(\mathbf{Y}|\boldsymbol{\Psi})$ is the likelihood function, that is, the conditional joint probability density function of the observed data $\mathbf{Y}$ given the parameter vector $\boldsymbol{\Psi}$, and $g(\mathbf{Y})$ denotes a fully specified standardizing term that is a function of the data alone (which thus has no impact on model selection). Based on the posterior distribution of $D(\boldsymbol{\Psi})$, DIC consists of two components as follows:

$$DIC = \bar{D} + p_D = 2\bar{D} - D(\bar{\boldsymbol{\Psi}}), \tag{8}$$

where $\bar{D} = E_{\boldsymbol{\Psi}|\mathbf{Y}}[D(\boldsymbol{\Psi})] = E_{\boldsymbol{\Psi}|\mathbf{Y}}[-2\log p(\mathbf{Y}|\boldsymbol{\Psi})]$ and $p_D = \bar{D} - D(\bar{\boldsymbol{\Psi}})$ is the effective number of parameters, defined as the difference between the posterior

mean of the deviance and the deviance evaluated at the posterior mean $\bar{\boldsymbol{\Psi}}$ of the parameters. As with other model selection criteria, we caution that DIC is not intended for identification of the 'correct' model, but rather merely as a method of comparing a collection of alternative formulations. In our model with different baseline characteristics and/or the MEMS adherence summary metrics, DIC can be used to identify the most significant covariate and MEMS adherence summary metrics in contribution to virologic response. Under the model (5), in the absence of any standardizing function $g(\mathbf{Y})$, the deviance is

$$
\begin{aligned}
D(\sigma^{-2}, \boldsymbol{\Theta}) &= -2\log p(\mathbf{Y}|\sigma^{-2}, \boldsymbol{\Theta}) \\
&= \sum_{i=1}^{n} \sigma^{-2}\big(\mathbf{y}_i - \mathbf{f}_i(\boldsymbol{\theta}_i)\big)^T\big(\mathbf{y}_i - \mathbf{f}_i(\boldsymbol{\theta}_i)\big) - \log\sigma^{-2}\sum_{i=1}^{n} m_i.
\end{aligned} \tag{9}
$$

As discussed above, our MCMC approach to estimating DIC first draws $\{(\sigma^{-2}, \boldsymbol{\Theta})^{(g)}\}_{g=1}^{G}$ values from the posterior distribution, and then calculates corresponding $\{D^{(g)}\}_{g=1}^{G}$ values from (9), where G is the number of samples of posterior distribution. Finally, we estimate DIC as $2\bar{D} - D(\bar{\sigma}^{-2}, \bar{\boldsymbol{\Theta}})$, where $\bar{D} = \frac{1}{G}\sum_{g=1}^{G} D^{(g)}$, $\bar{\sigma}^{-2} = \frac{1}{G}\sum_{g=1}^{G}(\sigma^{-2})^{(g)}$, $\bar{\theta}_i = \frac{1}{G}\sum_{g=1}^{G}\theta_i^{(g)}$ and $\bar{\boldsymbol{\Theta}} = \{\bar{\theta}_i, i = 1, \ldots, n\}$.

3. Analysis of AIDS clinical data.

3.1. *Motivating application and observed data.* The subject sample in our analysis was drawn from the AIDS Clinical Trials Group (ACTG) 398 study, a randomized, double-blind, placebo-controlled, 4-Arm trial study of amprenavir (APV) as part of several dual protease inhibitor (PI) regimens in subjects with HIV infection in whom initial PI therapy had failed. Subjects in all arms received APV (PI), three reverse transcriptase inhibitors (RTI): efavirenz (EFV), abacavir (ABC) and adefovir dipivoxil (ADV) plus a second PI or placebo: Arm A (saquinavir = SQV), Arm B (indinavir = IDV), Arm C (nelfinavir = NFV) and Arm D (placebo matched for one of these three PIs). Subjects are HIV-infected individuals with prior exposure to approved PIs and who have exhibited loss of virologic suppression as reflected by a plasma HIV-1 RNA concentration of $\geq$1000 copies/ml. Subjects were scheduled for follow-up visits at study (day 0), at weeks 2, 4, 8, 12, 16 and every 8 weeks thereafter until week 72, and at the time of confirmed virologic failure. More detailed descriptions of this study and data are given by Hammer et al. (2002) and Pfister et al. (2003).

As indicated previously, the primary objective of this paper is to investigate the effect of adherence interaction with drug resistance and baseline covariates to prescribed ARV therapy on virologic response measured repeatedly over time in HIV-infected patients. We construct a novel HIV dynamic model (which is parameter identifiable) with consideration of drug adherence assessed by use of MEMS data,

drug susceptibility (IC_{50}) and baseline covariates to link plasma drug concentration to the long-term changes in HIV-1 RNA observation after initiation of therapy. In the model we incorporate the two clinical factors (drug adherence measured by MEMS data and drug susceptibility) and baseline viral load and CD4 cell count into a function of treatment efficacy (see Section 2.2).

Because phenotype sensitivity testing was performed only on a subset of randomly selected subjects, the number of subjects available for our analysis was greatly reduced. We chose to consider only the subjects within Arm C for our analysis because this arm afforded the greatest number of subjects ($n = 31$) with available phenotypic drug susceptibility data on the two PIs (APV and NFV) and had available MEMS adherence data, as required for our model. A summary of measurements of data to be used in our analysis is briefly described below.

Plasma viral load: Plasma viral load was measured in copies/ml at designed study time by the ultrasensitive reverse transcriptase–polymerase chain reaction HIV-1 RNA assay (Roche Molecular Systems). Only measurements taken while on protocol-defined treatment were used in the analysis. The exact day of viral load measurement (not predefined study week) was used to compute study day in our analysis. A $\log_{10}$ transformation was used in the analysis of viral load data. The graph in Figure 1 (up-left panel) shows the viral load trajectories of those subjects. Note that some viral load measurements at designed study time were not observed due to laboratory and other problems (for example, viral load measurement was not observed at week 12 for the subject displayed in Figure 1).

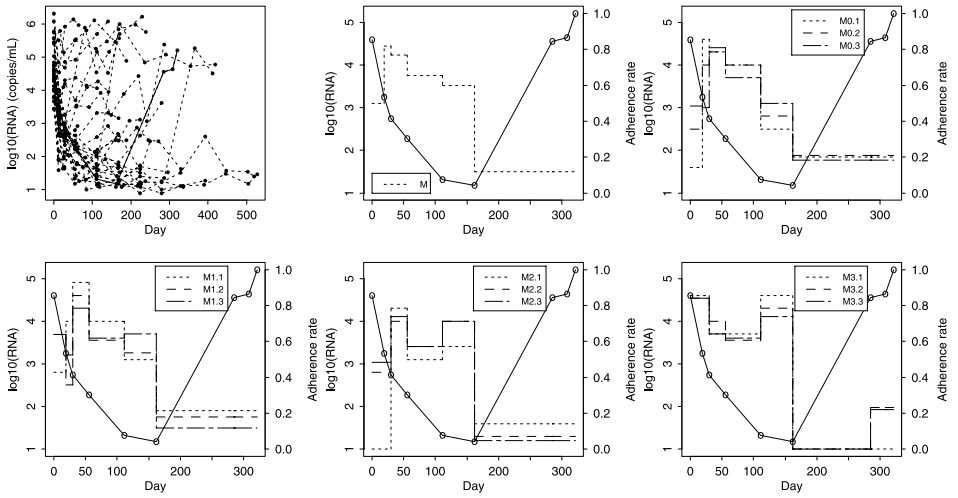

FIG. 1. *The profiles of viral load measurements* (*in* $\log_{10}$ *scale*) *from the* 31 *patients* (*up-left panel*) *and one trajectory of viral load* (*solid curve*) *and associated adherence rates* (*stairsteps*) *over time from the thirteen summary measures of MEMS data with the APV drug for one subject from ACTG*398.

Medication adherence: Medication adherence was measured by two methods: by the use of questionnaires and by the use of MEMS [Pfister et al. (2003)]. Subjects completed an adherence questionnaire at study weeks. The questionnaire was completed by the study participant and/or by a face-to-face interview with study personnel. For MEMS, an MEMS cap was used to monitor APV and EFV compliance only. The subjects were asked to bring their medication bottles and caps to the clinic at each study visit, where cap data were downloaded to computer files and stored for later analysis. The MEMS adherence rate for APV was determined as the sum of positive dosing events divided by the sum of prescribed dosing events during the specified time interval. In our analysis, we assumed that NFV had the same MEMS adherence rate as APV since both APV and NFV were prescribed with the same dosing schedule (twice daily), a prescribed AM and PM dosing period was defined for each subject and, hence, the bottles were opened twice per day [Pfister et al. (2003)]. As discussed previously, this study focuses mainly on investigating optimal strategy to summarize adherence rates determined by MEMS data for efficient production of virologic responses. For the MEMS data analysis, it was not possible to model daily adherence rates and instead the adherence rate was computed with the following scenarios to consider effects of both interval length and time frame (delay of timing) for MEMS assessment.

To determine the best summary metric of the MEMS adherence rate, we evaluated different assessment interval lengths (averaging adherence dosing events over 1, 2 or 3 week intervals) and different assessment time frames (fixing the assessment interval times to end either immediately or 1, 2 or 3 weeks prior to the next measured viral load). Table 1 summarizes the MEMS assessment interval notation and definitions for the 13 scenarios. As an example, M2.2 in Table 1 denotes an MEMS adherence interval length of 2 weeks fixed to end 2 weeks prior to the next viral load measurement; for instance, the MEMS adherence rate for a subject at study week 8 (day 56) was calculated as the number of nominal dosing events divided by the number of prescribed dosing events over study days 29–42 and this value was used to represent adherence from the previous study visit to the study visit at the day 56 for modeling. The case M serves as a reference and averages all the available MEMS data between viral load measurements. As an example, the viral load (in $\log_{10}$ scale) and adherence rates over time from the thirteen cases of MEMS data with APV drug for the one representative subject are presented in Figure 1.

Phenotypic virus susceptibility to drug: The phenotypic virus resistance to drug were retrospectively determined from baseline samples. Patients were selected to have samples assayed based on receiving study treatment for at least 8 weeks and having available sample. Some patients had virologic failure and phenotypic susceptibility testing done on samples at the time of failure. Testing was done via the recombinant virus assay (PhenoSense, ViroLogic Inc., South San Francisco, CA). For analysis, we used the phenotype marker, IC_{50} [Molla et al. (1996)], to quantify agent-specific drug resistance. We refer to this marker as the median inhibitory

TABLE 1
Summary of the MEMS interval definitions and other information

Case	MEMS adherence interval name	Adherence interval definition		Example for week 8 (day 56), adherence computed over days
		Time frame length (weeks prior to viral load measurement)	Interval length	
1	M	0 week	visit time	28–55
2	M0.1	0 week	1 week	49–55
3	M0.2	0 week	2 weeks	42–55
4	M0.3	0 week	3 weeks	35–55
5	M1.1	1 week	1 week	43–49
6	M1.2	1 week	2 weeks	36–49
7	M1.3	1 week	3 weeks	29–49
8	M2.1	2 weeks	1 week	36–42
9	M2.2	2 weeks	2 weeks	29–42
10	M2.3	2 weeks	3 weeks	22–42
11	M3.1	3 weeks	1 week	29–35
12	M3.2	3 weeks	2 weeks	22–35
13	M3.3	3 weeks	3 weeks	15–35

concentration. The baseline ($\circ$) and failure time ($\times$) IC_{50}'s of 31 subject-specific individuals for the APV and NFV drugs are displayed in Figure 2 (upper panel) and are used to construct $IC_{50}(t)$. Note that some subjects have only baseline IC_{50} due to the fact that they maintained viral suppression or dropped out from the study. If no IC_{50} measurement is observed at failure time for a subject, $IC_{50}(t)$ becomes a constant in this case.

Baseline characteristics: The baseline viral load in $\log_{10}$ scale (VL) and the baseline CD4 cell count were chosen as covariates in the model for data analysis. The log-transformation of viral load is used to stabilize the variance of measurement error and estimation algorithm. The baseline characteristics of 31 subject-specific individuals with mean, standard deviation (SD) and coefficient of variation (CV) are displayed in Figure 2 (lower panel). To avoid very small (large) estimates which may be unstable, we standardized these covariate values. For baseline $\log_{10}$(RNA), for instance, each $\log_{10}$(RNA) value is subtracted by mean (4.71) and divided by standard deviation (0.70).

3.2. *Model fitting and parameter estimation results.* In this section we apply the BNLME modeling approach to fit the data described in Section 3.1. Based on the discussion in Section 2, the prior distribution for $\boldsymbol{\mu}$ was assumed to be $\mathcal{N}(\boldsymbol{\eta}, \boldsymbol{\Lambda})$ with $\boldsymbol{\Lambda}$ being a diagonal matrix. Following the idea of Huang and Wu (2006) for prior construction, as an example we discuss the prior construction for $\log \delta$. The prior constructions for other parameters are similar and so are omitted here.

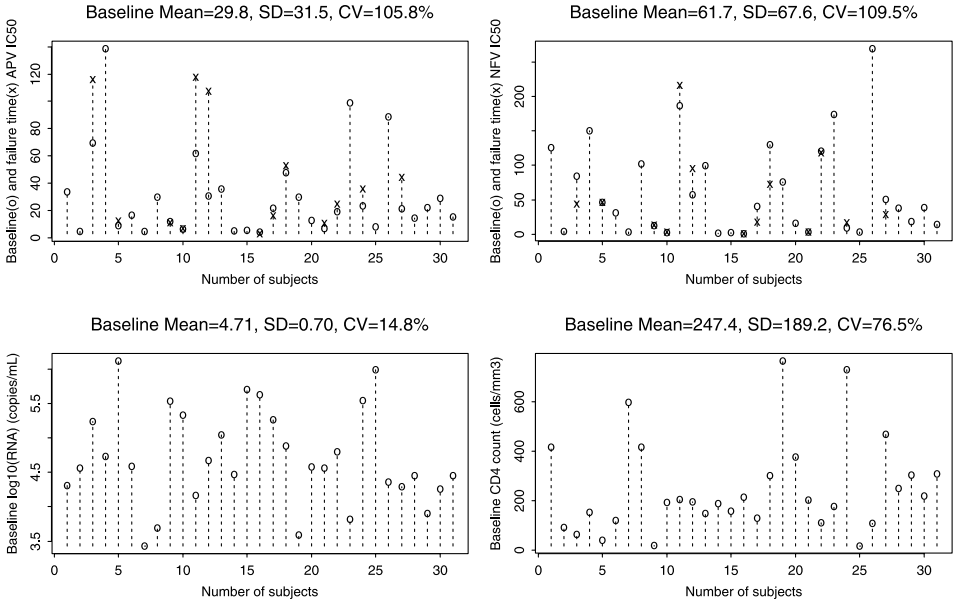

FIG. 2. *The baseline* (∘) *and failure time* (×) IC_{50} *for APV/NFV drugs* (*upper panel*) *with baseline* IC_{50} *mean*, *standard deviation* (*SD*) *and coefficient of variation* (*CV*), *respectively*, *and the baseline viral load in* $\log_{10}$ *scale and baseline CD*4 *cell count* (*lower panel*) *with mean*, *SD and CV*, *respectively*, *for the* 31 *subject-specific individuals from the ACTG*398 *study. Note that for a subject*, *if a single measurement of* IC_{50} *is observed at baseline only*, *there is no* × *sign appearing in the upper panel of the plot.*

Ho et al. (1995) reported viral dynamic data on 20 patients; the logarithm of the average death rate of infected cells ($\log \delta$) is -1.125. Wei et al. (1995) used two different models with a group of 22 subjects to estimate death rate of infected cells and obtained $\log \delta$ with -0.84 and -1.33, respectively. Following these two studies, Nowak et al. (1995) estimated $\log \delta = -0.934$ based on 11 subjects with one possible outlying subject excluded. It can be seen that four estimates of $\log \delta$ from these studies are -1.125, -0.84, -1.33 and -0.934, respectively. The individual estimates of $\log \delta$ from these studies approximately follow a symmetric normal distribution. Thus, we chose a normal distribution $\mathcal{N}(-1.0, 100.0)$ as the prior for $\log \delta$ (the large variance indicated that we used a noninformative prior for $\log \delta$). Similarly, the values of the hyper-parameters at population level are chosen as follows [Ho et al. (1995); Nowak et al. (1995); Nowak and May (2000); Perelson et al. (1996, 1997); Perelson and Nelson (1999); Verotta (2005); Wei et al. (1995)]:

$$a = 4.5, \qquad b = 9.0, \qquad \nu = 10.0,$$

$$\mathbf{\Lambda} = \operatorname{diag}(100.0, 100.0, 100.0, 100.0, 100.0, 100.0, 100.0, 100.0),$$

$$\boldsymbol{\eta} = (1.1, -1.0, -2.5, 1.2, 1.0, 1.0, 0.5, 0.5)^T,$$

$$\mathbf{\Omega} = \operatorname{diag}(2.5, 2.5, 2.5, 2.5, 2.5, 2.5).$$

We decide that one long chain is run for MCMC implication with considerations of the following two issues: (i) a number of initial "burn-in" simulations are discarded, since from an arbitrary starting point it would be unlikely that the initial simulations came from the stationary distribution targeted by the Markov chain; (ii) one may only save every kth (k being an integer) simulation sample to reduce the dependence among samples used for parameter estimation. Because the antiviral response modeling involves numerically solving nonlinear differential equations, thus computational burdens would be more pronounced with the Bayesian approaches via MCMC procedure. Utilizing efficient computer algorithms are critical in this regard. Therefore, we are going to adopt these strategies in our MCMC implementation using FORTRAN code that calls a differential equation subroutine solver (DIVPRK) in the IMSL library (1994), which uses the Runge–Kutta–Verner fifth-order method. The computer codes are available from the corresponding author upon request. An informal check of convergence is conducted based on graphical techniques according to the suggestion of Gelfand and Smith (1990). Based on the results, we propose that, after an initial number of 20,000 burn-in iterations, every 4th MCMC sample was retained from the next 80,000 samples. Thus, we obtained 20,000 samples of targeted posterior distributions of the unknown parameters.

We fitted the model to the data from 31 subjects discussed in Section 3.1 using the proposed BNLME modeling approach. We incorporate the two clinical factors, drug adherence assessed by MEMS cap data and drug susceptibility (phenotype IC_{50} values), as well as baseline covariates into a function of drug efficacy. For model fitting, adherence rates were determined from MEMS data with 13 different scenarios. For model fitting and the purpose of comparisons, we set up a control model as the one without using any drug adherence, resistance and covariate information which corresponds to setting $\gamma(t) = 2/(\exp(\beta_0) + 2)$ with $IC_{50}(t) = 1$, $A(t) = 1$ and $w_1 = w_2 = 0$; for this case, our model reverts to that discussed by Nowak and May (2000) and Perelson and Nelson (1999). The other 13 models are specified based on the combination of drug resistance (IC_{50}), baseline covariate data and 13 different adherence summary metrics listed in Table 1.

In order to assess how adherence rates, determined from 13 different scenarios, interacted with drug susceptibility and covariates to contribute to virologic response, we fitted the models to all 13 scenarios as well as the control model and compared the fitting results. We found based on the DIC criterion (see Figure 3) that, overall, the model with adherence rate determined from MEMS dosing events, taken time frame length of 2 weeks prior to a viral load measurement with over either a 2 week assessment interval (M2.2) or a 3 week assessment interval (M2.3), provided the best fits to the observed data, compared to the other 12 models for most subjects. The reference model with adherence rate averaged by all the available MEMS data between viral load measurements gave a moderate fit to the observed data. We clearly see that all models fit the early viral load data well, but the control model, lacking factors for subject-specific drug adherence

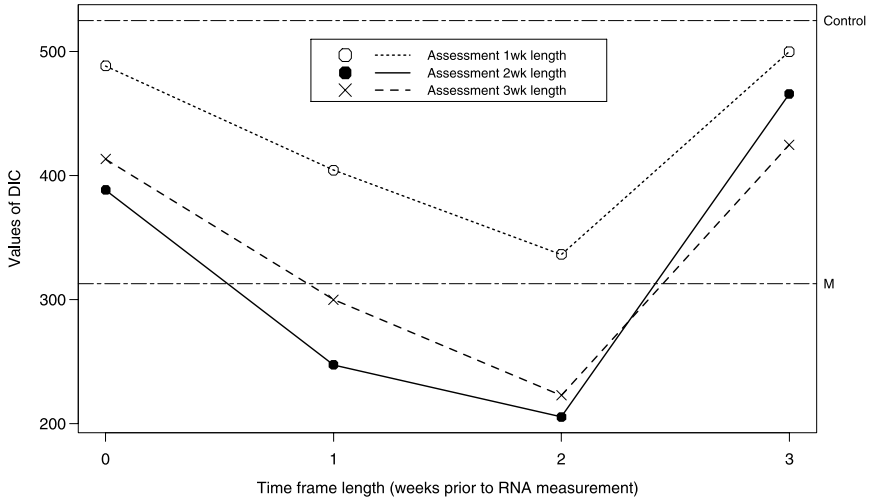

FIG. 3. *Comparison of the DIC values for the models from* 13 *different determinants of MEMS adherence*, *interacted by drug resistance and covariates*, *with the control model*. *The two horizontal lines represent the DIC values for the control model and the reference model with adherence rate determined by case M*, *respectively.*

and susceptibility as well as baseline covariates, failed to fit viral load rebounds and fluctuations, and provided the worst fitting results for the majority of subjects. For the purpose of illustration, the model fitting curves from the control model (solid curves), the best fit model (M2.2: dotted curves) and the reference model (M: dashed curves) are displayed in Figure 4 for the three representative subjects.

For the purpose of comparison, Figure 5 presented the population posterior means and the corresponding 95% equal-tail credible intervals (CI) of the eight

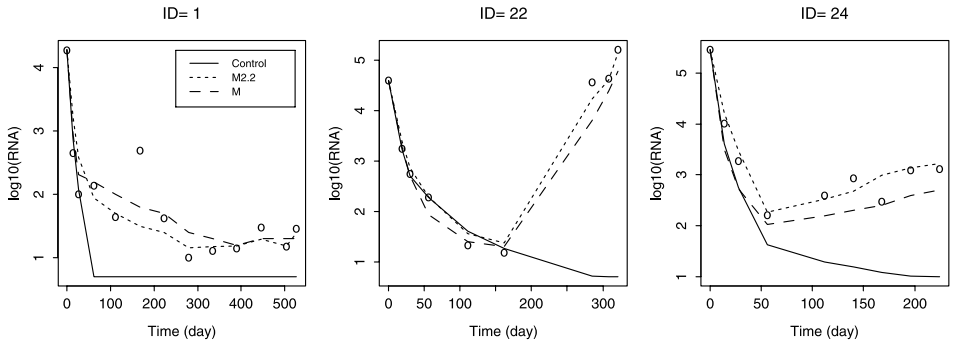

FIG. 4. *The estimate of viral load trajectory from the model fitting with the* 3 *different determinants of adherence*: (i) *Control model* (*solid curves*), (ii) *M*2.2 *model* (*dotted curves*) *and* (iii) *reference* (*M*) *model* (*dashed curves*) *for the three representative subjects*. *The observed values are indicated by circles*.

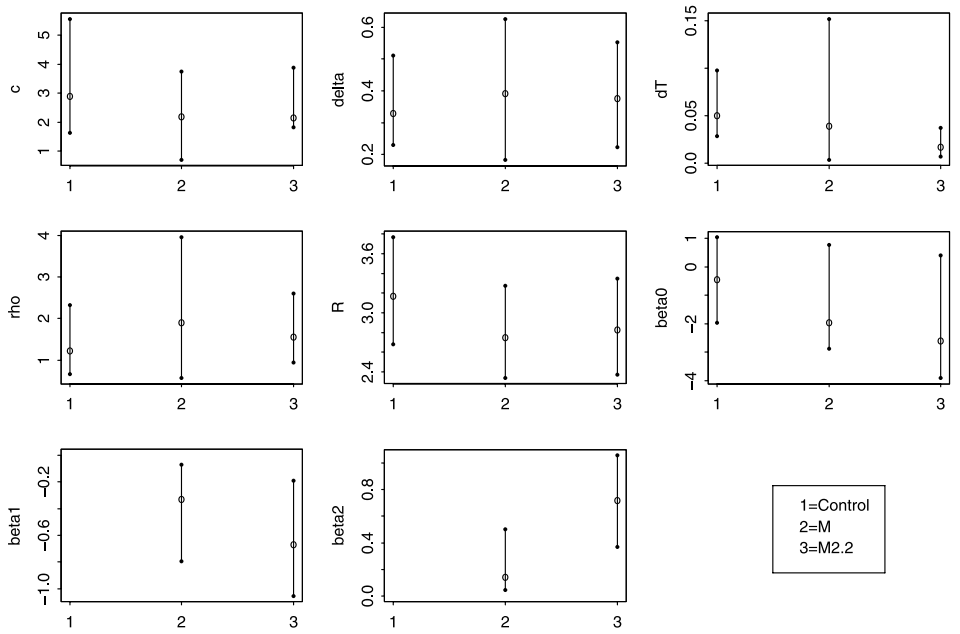

FIG. 5. *A summary of the estimated posterior means* (○) *of population parameters and the corresponding* 95% *equal-tail credible intervals* (*CI*) *for the models from* 3 *different determinants of adherence.*

parameters for the control model, the best fit model (M2.2) and the reference model (M). For the six dynamic parameters $(c, \delta, d_T, \rho, R, \beta_0)$, it is shown that the population estimates for the control model have higher clearance rate of free virions (c), lower death rate of infected cells (δ), higher death rate of target T cells (d_T), smaller viral load scaling factor (ρ), higher basic reproductive ratio for the virus (R) and larger ϕ than those for the best fit model (M2.2) and reference model (M), while the population estimates for the best fit model and reference model are generally similar. These differences may result from the effects of drug adherence interacted with drug resistance and covariates in the models. For the other two covariate effect parameters (β_1, β_2) which are relevant to treatment effect, we will discuss them separately in Section 3.4. In terms of the individual parameter estimates, a large between-subject variation in the estimates of all individual dynamic parameters was observed (data not shown here). Overall, the coefficient of variation ranges from 15.4% to 88.9% for all parameters.

3.3. *Effects of adherence rates determined by different MEMS summary metrics*. Figure 3 in Section 3.2 displayed a comparison of the DIC values for the models from 13 different determinants of MEMS adherence, interacted by drug resistance and covariates, with the control model. The observed patterns shown in Figure 3 provided information to answer the following questions: (i) what MEMS

assessment interval length is best and (ii) what MEMS assessment time frame (delay effect of timing) is best?

We can see that when the time frame for MEMS assessment is fixed, models with a 2 week MEMS assessment interval length generally outperform models with an assessment interval length of 1 or 3 weeks except for the time frame length with 3 weeks prior to viral load measurement where the model with a 3 week MEMS assessment interval length performs best.

Regardless of the assessment interval length, models which assess compliance 2 weeks prior to viral load measurement generally outperform models which assess compliance immediately before viral load measurement, 1 week before or 3 weeks before viral load measurement. Overall, the model with a MEMS assessment interval length of 2 weeks measured from 4 to 2 weeks prior to viral load measurement (M2.2) was significantly a better predicator of viral load over time than any other models, with the exception of the M2.3 model which shows no significant difference from the M2.2 model in terms of DIC values.

3.4. *Treatment effects of baseline characteristics interacted with clinical factors*. Figure 5 summarized the population posterior means and the corresponding 95% equal-tail CI of the covariate effect parameters β_1 and β_2 for the best fit model (M2.2) and the reference model (M). It can be seen that estimates of β_1 (coefficient of baseline viral load) are negative, while estimates of β_2 (coefficient of baseline CD4 cell count) are positive. In fact, other models also provided the same scenarios for the estimates of these two parameters (not shown here). As an example, we report results based on the best fit model (M2.2). We can observe from Figure 5 that the estimates of β_1 and β_2 are $\hat{\beta}_1 = -0.67$ with 95% CI $(-1.056, -0.193)$ and $\hat{\beta}_2 = 0.719$ with 95% CI (0.371, 1.058). It indicates that, according to antiviral drug efficacy model (4), the baseline viral load ($\hat{\beta}_1 = -0.67$) has a significant positive effect on drug efficacy $\gamma(t)$, while the baseline CD4 cell count ($\hat{\beta}_2 = 0.719$) has a significant negative effect on $\gamma(t)$ since the corresponding 95% credible intervals do not contain zero for both parameters. These findings could suggest us with the following different ways. The lowest value of $\gamma(t)$ [highest ϕ as displayed in Figure 6(b)] occurs in the subjects with the best prognosis (higher baseline CD4 cell count and lower baseline viral load). Alternatively, the highest value of $\gamma(t)$ (lowest ϕ) occurs in those with the worst prognosis (lower baseline CD4 cell count and higher baseline viral load). A possible explanation is that there is a floor effect of viral load (or ceiling/floor effect of CD4 cell count) that is not captured in the model. Further, given that baseline CD4 cell count and viral load are jointly used to make treatment decisions and are known to be negatively correlated as shown in Figure 6(a), the result based on the combination of baseline viral load and CD4 count in $\gamma(t)$ indicates that the baseline CD4 cell count and viral load have the opposite effect on drug efficacy which might be intuitively understandable.

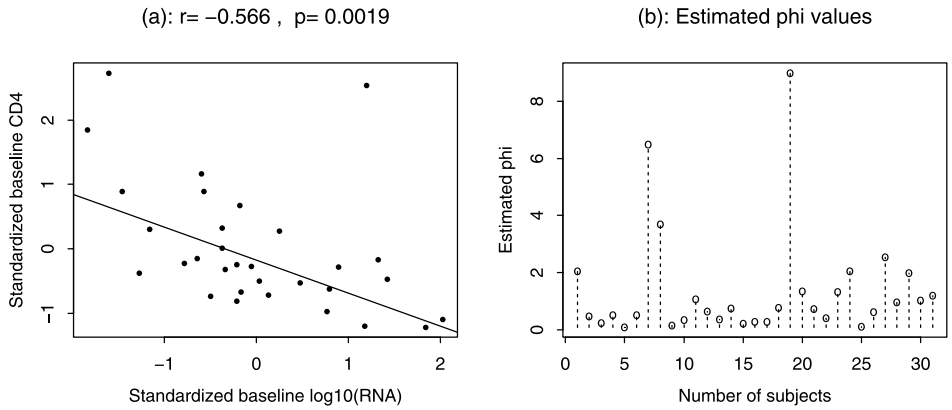

FIG. 6. (a) *Correlation between* (*standardized*) *baseline* $\log_{10}$(*RNA*) *and CD*4 *cell count. The correlation coefficient* (r) *and p-value are obtained from the Spearman rank correlation test. The line is a robust* (*MM-estimator*) *linear regression fit*. (b) *Estimated* ϕ *values for the* 31 *subject-specific individuals*.

4. A simulation study. In this paper we investigated the association between virologic outcomes and medication adherence with confounding factors based on the data from 31 subjects. As both one referee and the associate editor suggested that a simulation study may be useful to evaluate how our method performs, in this section we conduct a limited simulation study here due to intensive computations involved. The scenario we consider is as follows.

We simulate a clinical trial with 31 patients receiving antiviral treatment. For each patient, we assume that the designs of this experiment, in particular, the sampling times for viral load, were the same as those in the ACTG 398 study. The data for the phenotype marker (baseline and failure IC_{50}'s), medication adherence and the baseline viral load/CD4 cell count were taken from the ACTG 398 study, where medication adherence was calculated by the M2.2 summary measure. The "true" values of unknown parameters were the same as those estimated from the data set of 31 subjects which were reported in Section 3. With generated individual true parameters based on the equation (6), known data $[IC_{50}(t), A(t), w_1$ and $w_2]$, we generated random samples for response (viral load) based on model (2). The values of hyper-parameters are chosen to be the same as those in Section 3. For each simulated data set, we fit the model using the Bayesian approach. The MCMC techniques consisting of a series of Gibbs sampling and M–H algorithms were the same as those in the real data analysis. We performed 50 replications and obtained the mean estimates (ME) of population parameters together with the corresponding relative bias (RB), which is the difference between the mean estimate and the true value of the parameter divided by absolute value of the true parameter, and the standard error (SE), defined as the square root of mean-squared error divided by the absolute value of the true parameter.

TABLE 2

The true values (TV) of parameters and mean estimates (ME) of population parameters with 50 replications as well as the corresponding relative bias (RB), defined as $100 \times (ME - TV)/|TV|$, *and standard error (SE), defined as* $100 \times \sqrt{MSE}/|TV|$

Parameter	TV	ME	RB (%)	SE (%)
$\log c$	0.767	0.771	0.522	9.127
$\log \delta$	−0.977	−1.013	−3.685	7.971
$\log d_T$	−4.086	−4.101	−0.367	5.871
$\log \rho$	0.433	0.388	−10.39	18.03
$\log R$	1.040	1.100	5.769	3.089
β_0	−2.615	−2.604	0.421	4.902
β_1	−0.670	−0.665	0.746	10.13
β_2	0.719	0.698	−2.921	13.09

In Table 2 we summarize the true values (TV) of parameters and the ME of population parameters with 50 replications as well as the corresponding RB and SE. The percentage is based on the absolute value of the true parameter. It can be seen from Table 2 that the RB (%) for population parameter estimates are very small, ranging from 0.522 to 10.39, and the SE (%) ranges from 3.089 to 18.03. The simulation results indicate that our method with considering the M2.2 model performs reasonably well in terms of estimates of parameters except for the viral load proportionality factor $\log \rho$ which has larger RB and SE. That is, our method produces a substantially biased estimate and may severely underestimate $\log \rho$. This may be explained by the fact that it is probably caused from inaccurate numerical solutions to the system of ODE (2) which was used to construct the BNLME model.

5. Concluding discussion. In developing long-term dynamic modeling, this paper introduced a dynamic mechanism specified by a system of time-varying ODE to (i) establish a link between success of ARV therapy in virologic response and MEMS adherence confounded by drug resistance and baseline covariates, (ii) fully integrate viral load, MEMS adherence, drug resistance and baseline covariates data into the statistical inference and analysis, and (iii) provide a powerful tool to evaluate the effects of MEMS adherence determined by a different summary metric on virologic response using the BNLME modeling approach. This approach cannot only combine prior information with current clinical data for estimating dynamic parameters, but also deal with complex dynamic systems. Thus, the results of estimated dynamic parameters based on this model should be more reliable and reasonable to interpret long-term HIV dynamics. Our models are simplified with the main goals of retaining crucial features of HIV dynamics and, at the same time, guaranteeing their applicability to typical clinical data, in particular, long-term viral load measurements. The proposed model fitted the clinical data reasonably well for most patients in our study, although the fitting for a few

patients was not completely satisfactory because of unusual viral load fluctuation patterns for these subjects.

We have explored the practical performance of DIC for the comparison of developed models. DIC, a Bayesian version of the classical deviance for model assessment, is particularly suited to compare Bayesian models whose posterior distribution has been obtained using MCMC procedures and can be used in complex hierarchical models where the number of unknowns often exceeds the number of observations and the number of free parameters is not well defined. This is in contrast to AIC and BIC, where the number of free parameters needs to be specified [Zhu and Carlin (2000)]. Overall, combined with more traditional residual analysis and posterior predictive model checks as discussed in this paper, DIC appears to offer a comprehensive framework for comparison and evaluation within a complex model class.

Several studies investigated the association between virologic responses and adherence assessed by MEMS data only without considering other confounding factors such as drug resistance using standard modeling methods including Poisson regression [Knafl et al. (2004)], logistic regression [Vrijens et al. (2005)] and the linear mixed-effects model [Liu et al. (2007)]. In this article we employed the proposed dynamic model and associated BNLME modeling approach to assessment of effects of adherence determinants based on MEMS dosing events in predicting virologic response. In particular, we investigated (i) how to summarize the MEMS adherence data for efficient prediction of virological response after accounting for potential confounding factors such as drug resistance and baseline covariates, and (ii) how to evaluate treatment effect of baseline characteristics interacted with MEMS adherence and other clinical factors. Note that a further study in comparing the performance of these different methods may be important and warranted, although some challenges are observed in terms of different model structures and data characteristics.

The results indicate that the best summary metric for prediction of virologic response based on DIC criterion is the adherence rate determined by MEMS dosing events averaged over an assessment interval of 2 or 3 weeks, and 2 weeks prior to the next measured viral load observation (denoted by M2.2 or M2.3). We found that the best MEMS adherence predictor (M2.2) of the effectiveness of ARV medications on virologic response is consistent with that reported in Huang et al. (2008) in which, however, the next best MEMS adherence predictor (M1.2) is different from what is obtained in this paper. This difference may be due to the various reasons as follows. In the study by Huang et al. (2008), (i) it directly applied the model (1) to fit data and, thus, some assumptions were made due to parameter unidentifiable issues; (ii) the analysis used the mean of the sum of squared deviations as a criterion to evaluate model fitting results; (iii) it assumed IC_{50} data were extrapolated linearly to the whole treatment period instead of a log-linear extrapolation offered in this paper which is considered more reasonable biologically; and

(iv) it did not incorporate baseline covariates in the model. In addition, the superiority of the M2.2 model, associated with the MEMS adherence rate based on time frame length of 2 weeks prior to a viral load measurement with over a 2 week assessment interval, may be explained by the fact that it probably reflects how long it takes for resistance mutations to first arise and then come to dominate the plasma population of a virus. As pointed out by an anonymous referee, this finding may also be interpreted as follows. Low adherence two weeks prior to the viral load measurement may not have had sufficient time for viral rebound to occur.

In this paper we set up a connection between subject-specific baseline characteristics with interaction of clinical factors and drug efficacy. We also found that, according to antiviral drug efficacy model (4), the baseline viral load had a positive effect on drug efficacy, while the baseline CD4 cell count had a negative effect on it. Our results may be explained by the fact that for those patients with higher baseline viral load, the drug efficacy needs to be higher than that for those with lower baseline viral load. Therefore, a strong treatment is recommended for those patients with higher baseline viral load. On the other hand, patients with higher CD4 cell count may need lower drug efficacy so that a more potent ARV drug regimen is not necessary for these patients to avoid side-effects of drug use. The results may suggest the benefit of initiating ARV therapy with a lower baseline viral load and/or a higher baseline CD4 count. These results coincide with those investigated by Notermans et al. (1998) and Wu et al. (2005) whose results were obtained using correlation analysis. Note that given the estimated parameters, the subject with both a high baseline CD4 cell count and a relatively high baseline viral load [upper right quadrant of Figure 6(a)] has a very different ϕ than that with a similar baseline CD4 cell count, but a low baseline viral load [upper left quadrant of Figure 6(a)]. It is possible that the subject in the upper right quadrant was more recently infected (hence the higher baseline CD4 cell count) or perhaps with a drug resistant virus and would not be a candidate for a regimen with a "less potent drug efficacy."

Our findings need to be interpreted in light of the study limitations. First, in the ACTG 398 study, because phenotype sensitivity testing was performed only on a subset of randomly selected subjects, we chose 31 patients who have available data for analysis in this paper. Second, due to reasons such as lost caps and malfunction of caps, there were inaccurate MEMS data across the treatment period which may not reflect actual adherence profile for individual patients and, thus, the data quality could have some impact on the results. Third, because of technical limitations, the undetectable values of viral load were replaced with 25 copies/ml for analyses, which could introduce some bias due to a cluster of ties of data points. Finally, this paper combined new technologies in mathematical modeling and statistical inference with advances in HIV/AIDS dynamics and ARV therapy to quantify complex HIV disease mechanisms. The complex nature of HIV/AIDS ARV therapy will naturally pose some challenges including missing data and measurement error in clinical factors and covariates. These complicated problems, which are beyond the

scope of this article, may be addressed, for example, using the joint model method [Wu (2002)] and other techniques [Carroll et al. (1995)], and are warranted for further investigation. Nevertheless, these limitations would not offset the major findings from this study.

As the Associate Editor pointed out, we assumed that the distributions of the random error and random effects are normal, which is a common assumption in the literature for statistical inference. However, due to the nature of AIDS clinical data, it is possible that the data may contain outliers and/or depart from normality and, thus, statistical inference and analysis with normal assumption may lead to misleading results [Verbeke and Lesaffre (1996); Ghosh et al. (2007)]. Specially non-normal characteristics such as skewness with heavy right or left tail may appear often in virologic responses. Thus, a normality assumption may be too restrictive to provide an accurate representation of the structure that is often present in repeated measures and clustered data. Thus, it is of practical interest to investigate nonlinear models with a skew-normal distribution or t distribution for (within-subject) random error and random effects which are more robust to outliers and skewness than those with a normal distribution. In our recent study [Huang and Dagne (2010)] we addressed a Bayesian approach to nonlinear mixed-effects models in conjunction with the HIV dynamic model and relaxed the normality assumption by considering both random error and random-effects to have a multivariate skew-normal distribution. The proposed model provides flexibility in capturing a broad range of non-normal behavior and includes normality as a special case. The results suggest that it is very important to assume models with a skew-normal distribution in order to achieve robust and reliable results, in particular, when the data exhibit skewness. We are actively applying this methodology into the data investigated in this paper and will report the results in a future study.

In summary, the mechanism-based dynamic model is powerful and efficient to characterize relations between antiviral response and medication adherence, drug susceptibility as well as baseline characteristics, although some biological assumptions are required. It is important to find a way to incorporate subject-specific information with regard to drug susceptibility, medication adherence and baseline characteristics in predicting long-term virologic response. Since each of these factors may only contribute a very small portion to virologic response and they may be confounded through complicated interactions, the appropriate modeling of the combination effects of these factors is critical to efficiently utilize the information in virologic response predictions. The viral dynamic model and associated statistical approaches discussed here provide a good avenue to fulfill this goal. In particular, MEMS adherence rate summarized by an optimal way in terms of assessing both interval lengths and time frame lengths prior to viral load measurement is an important factor that significantly determines the effectiveness of ARV treatment and needs to be taken into account in analysis of virologic responses. Our results demonstrate that MEMS adherence data may not predict virologic response well unless the MEMS cap data are summarized in an appropriate way as reported in

Section 3.3. Additionally, although this paper concentrated on HIV dynamics, the basic concept of longitudinal dynamic systems and the proposed methodologies in this paper are generally applicable to dynamic systems in other fields such as biology, medicine, engineering or PK/PD studies as long as they meet the relevant technical specification—a system of ODE.

Acknowledgments. The authors are extremely grateful to the Editor, an Associate Editor and one referee for their insightful comments and constructive suggestions that led to an improvement of the article. We gratefully acknowledge ACTG 398 study investigators for allowing us to use the clinical data from their study. The authors are indebted to Dr. Susan L. Rosenkranz from Frontier Science & Technology Research Foundation and SDAC of Harvard School of Public Health for her informative discussions and data preparations.

REFERENCES

ACOSTA, E. P., WU, H., WALAWANDER, A., ERON, J., PETTINELLI, C., YU, S., NEATH, D., FERGUSON, E., SAAH, A. J., KURITZKES, D. R., GERBER, J. G., FOR THE ADULT ACTG 5055 PROTOCOL TEAM (2004). Comparison of two indinavir/ritonavir regimens in treatment-experienced HIV-infected individuals. *Journal of Acquired Immune Deficiency Syndromes* **37** 1358–1366.

AKAIKE, H. (1973). Information theory and an extension of the maximum likelihood principle. In *2nd International Symposium on Information Theory* (B. N. Petrov and F. Csáki, eds.) 267–281. Akadémiai Kiadó, Budapest. MR0483125

ARNSTEN, J. H., DEMAS, P. A., FARZADEGAN, H. ET AL. (2001). Antiretroviral therapy adherence and viral suppression in HIV-infected drug users: Comparison of self-report and electronic monitoring. *Clin. Infect. Dis.* **33** 1417–1423.

BONHOEFFER, S., LIPSITCH, M. and LEVIN, B. R. (1997). Evaluating treatment protocols to prevent antibiotic resistance. *Proc. Natl. Acad. Sci. USA* **94** 12106–12111.

BONHOEFFER, S., MAY, R. ET AL. (1997). Viral dynamics and drug therapy. *Proc. Natl. Acad. Sci. USA* **94** 6971–6976.

BOVA, C. A., FENNIE, K. P., KNAFL, G. J. ET AL. (2005). Use of electronic monitoring devices to measure antiretroviral adherence: Practical considerations. *AIDS Behav.* **9** 103–110.

CARROLL, R. J., RUPPERT, D. and STEFANSKI, L. A. (1995). *Measurement Error in Nonlinear Models*. Chapman and Hall, London. MR1630517

COBELLI, C., LEPSCHY, A. and JACUR, G. R. (1979). Identifiability of compartmental systems and related structural properties. *Math. Biosci.* **44** 1–18. MR0553871

DAVIDIAN, M. and GILTINAN, D. M. (1995). *Nonlinear Models for Repeated Measurement Data*. Chapman and Hall, London.

GABRIELSSON, J. and WEINER, D. (2000). *Pharmacokinetic and Pharmacodynamic Data Analysis: Concepts and Applications*. Apotekarsocieteten, Stockholm.

GAMERMAN, D. (1997). *Markov Chain Monte Carlo: Stochastic Simulation for Bayesian Inference*. Chapman and Hall, London. MR2260716

GELFAND, A. E. and SMITH, A. F. M. (1990). Sampling-based approaches to calculating marginal densities. *J. Amer. Statist. Assoc.* **85** 398–409. MR1141740

GHOSH, P., BRANCO, M. D. and CHAKRABORTY, H. (2007). Bivariate random effect model using skew normal distribution with application to HIV-RNA. *Statist. Med.* **26** 1255–1267. MR2345719

GILKS, W. R., RICHARDSON, S. and SPIEGELHALTER, D. J., EDS. (1995). *Markov Chain Monte Carlo in Practice*. Chapman and Hall, London. MR1397966

HAMMER, S. M., VAIDA, F. ET AL. (2002). Dual vs single protease inhibitor therapy following antiretroviral treatment failure: A random trial. *J. Amer. Med. Assoc.* **288** 169–180.

HAN, C., CHALONER, K. and PERELSON, A. S. (2002). Bayesian analysis of a population HIV dynamic model. In *Case Studies in Bayesian Statistics* (C. Gatsoiquiry, R. E. Kass, A. Carriquiry, A. Gelman, D. Higdon, D. K. Pauler and I. Verdinellinis, eds.) **6** 223–237. Springer, New York. MR1959658

HAUBRICH, R. H., LITTLE, S. J., CURRIER, J. S. ET AL. (1999). The value of patient-reported adherence to antiretroviral therapy in predicting virologic and immunologogic response. *AIDS* **13** 1099–1107.

HO, D. D., NEUMANN, A. U., PERELSON, A. S., CHEN, W., LEONARD, J. M. and MARKOWITZ, M. (1995). Rapid turnover of plasma virions and CD4 lymphocytes in HIV-1 infection. *Nature* **373** 123–126.

HUANG, Y. and DAGNE, G. (2010). Skew-normal Bayesian nonlinear mixed-effects models with application to AIDS studies. *Statist. Med.* **29** 2384–2398.

HUANG, Y., HOLDEN-WILTSE, J., ROSENKRANZ, S. L., ERON, J. J., HAMMER, S. M., MELLORS, J. W. and WU, H. (2008). Modeling adherence of protease inhibitors for prediction of virologic response in HIV-1 infected patients: Comparison between adherence measurements by MEMS and questionnaire. Technical report, Department of Epidemiology and Biostatistics, Univ. South Florida, Tampa, FL.

HUANG, Y., LIU, D. and WU, H. (2006). Hierarchical Bayesian methods for estimation of parameters in a longitudinal HIV dynamic system. *Biometrics* **62** 413–423. MR2227489

HUANG, Y., ROSENKRANZ, S. L. and WU, H. (2003). Modeling HIV dynamics and antiviral responses with consideration of time-varying drug exposures, sensitivities and adherence. *Math. Biosci.* **184** 165–186. MR1991484

HUANG, Y. and WU, H. (2006). A Bayesian approach for estimating antiviral efficacy in HIV dynamic model. *J. Appl. Statist.* **33** 155–174. MR2223142

ICKOVICS, J. R. and MEISLER, A. W. (1997). Adherence in AIDS clinical trial: A framework for clinical research and clinical care. *J. Clin. Epid.* **50** 385–391.

IMSL MATH/LIBRARY (1994). *FORTRAN Subroutines for Mathematical Applications*, Vol. 2. Visual Numerics, Houston.

KASTRISSIOS, H., SUAREZ, J. R., KATZENSTEIN, D. ET AL. (1998). Characterizing patterns of drug-taking behavior with a multiple drug regimen in an AIDS clinical trial. *AIDS* **12** 2295–2303.

KNAFL, G. J., FENNIE, K. P., BOVA, C. ET AL. (2004). Electronic monitoring device event modeling on an individual-subject basis using adaptive Poisson regression. *Statist. Med.* **23** 783–801.

LABBÉ, L. and VEROTTA, D. (2006). A nonlinear mixed effect dynamic model incorporating prior exposure and adherence to treatment to describe long-term therapy outcome in HIV-patients. *J. Pharmacokinet. Pharmacodyn.* **33** 519–542.

LEVINE, A. J., HINKIN, C. H., MARION, S. ET AL. (2006). Adherence to antiretroviral medications in HIV: Differences in data collected via self-report and electronic monitoring. *Health Psychol.* **25** 329–335.

LIU, H., MILLER, L. G., GOLIN, C. E. ET AL. (2007). Repeated measures analyses of dose timing of antiretroviral medication and its relationship to HIV virologic outcomes. *Statist. Med.* **26** 991–1007. MR2339229

MOLLA, A., KORNEYEVA, M. ET AL. (1996). Ordered accumulation of mutations in HIV protease confers resistance to ritonavir. *Nat. Medic.* **2** 760–766.

NOTERMANS, D. W., GOUDSMIT, J., DANNER, S. A. ET AL. (1998). Rate of HIV-1 decline following antiretroviral therapy is related to viral load at baseline and drug regimen. *AIDS* **12** 1483–1490.

NOWAK, M. A., BONHOEFFER, S., CLIVE, L., BALFE, P., SEMPLE, M., KAYE, S., TENANT-FLOWERS, M. and TEDDER, R. (1995). HIV results in the frame. *Nature* **375** 193.

NOWAK, M. A., LLOYD, A. ET AL. (1997). Viral dynamics of primary viremia and antiretroviral therapy in simian immunodeficiency virus infection. *J. Virol.* **71** 7518–7525.

NOWAK, M. A. and MAY, R. M. (2000). *Virus Dynamics: Mathematical Principles of Immunology and Virology*. Oxford Univ. Press, Oxford. MR2009143

PATERSON, D. L., SWINDELLS, S., MOHR, J., BRESTER, M., VERGIS, E. N., SQULER, C., WAGENER, M. M. and SINGH, N. (2000). Adherence to protease inhibitor therapy and outcomes in patients with HIV infection. *J. Internal Med.* **133** 21–30.

PERELSON, A. S., NEUMANN, A. U., MARKOWITZ, M., LEONARD, J. M. and HO, D. D. (1996). HIV-1 dynamics in vivo: Virion clearance rate, infected cell life-span, and viral generation time. *Science* **271** 1582–1586.

PERELSON, A. S., ESSUNGER, P., CAO, Y., VESANEN, M., HURLEY, A., SAKSELA, K., MARKOWITZ, M. and HO, D. D. (1997). Decay characteristics of HIV-1-infected compartments during combination therapy. *Nature* **387** 188–191.

PERELSON, A. S. and NELSON, P. W. (1999). Mathematical analysis of HIV-1 dynamics in vivo. *SIAM Rev.* **41** 3–44. MR1669741

PFISTER, M., LABBE, L., HAMMER, S. M., MELLORS, J., BENNETT, K. K., ROSENKRANZ, S. L. and SHEINER, L B. and AIDS CLINICAL TRIAL GROUP PROTOCOL 398 INVESTIGATORS (2003). Population Pharmacokinetics and Pharmacodynamics of Efavirenz, Nelfinavir, and Indinavir: Adult AIDS Clinical Trial Group Study 398. *Antimicrobial Agents and Chemoterapy* **47** 130–137.

SCHWARZ, G. (1978). Estimating the dimension of a model. *Ann. Statist.* **6** 461–464. MR0468014

SPIEGELHALTER, D. J., BEST, N. G., CARLIN, B. P. and VAN DER LINDE, A. (2002). Bayesian measures of model complexity and fit. *J. Roy. Statist. Soc. Ser. B* **64** 583–639. MR1979380

STAFFORD, M. A. ET AL. (2000). Modeling plasma virus concentration during primary HIV infection. *J. Theoret. Biol.* **203** 285–301.

VERBEKE, G. and LESAFFRE, E. (1996). A linear mixed-effects model with heterogeneity in random-effects population. *J. Amer. Statist. Assoc.* **91** 217–221.

VEROTTA, D. (2005). Models and estimation methods for clinical HIV-1 data. *J. Comput. Appl. Math.* **184** 275–300. MR2160068

VRIJENS, B., GOETGHEBEUR, E., DE KLERK, E., RODE, R., MAYER, S. and URQUHART, J. (2005). Modeling the association between adherence and viral load in HIV-infected patients. *Statist. Med.* **24** 2719–2731. MR2196210

WAINBERG, M. A. ET AL. (1996). Effectiveness of 3TC in HIV clinical trials may be due in part to the M184V substition in 3TC-resistant HIV-1 reverse transcriptase. *AIDS* **10**(Suppl.), S3–S10.

WAKEFIELD, J. C., SMITH, A. F. M., RACINE-POON, A. and GELFAND, A. E. (1994). Bayesian analysis of linear and non-linear population models using the Gibbs sampler. *Appl. Statist.* **43** 201–221.

WAKEFIELD, J. C. (1996). The Bayesian analysis to population pharmacokinetic models. *J. Amer. Statist. Assoc.* **91** 62–75.

WEI, X., GHOSH, S. K., TAYLOR, M. E., JOHNSON, V. A., EMINI, E. A., DEUTSCH, P., LIFSON, J. D., BONHOEFFER, S., NOWAK, M. A., HAHN, B. H., SAAG, M. S. and SHAW, G. M. (1995). Viral dynamics in human immunodeficiency virus type 1 infection. *Nature* **373** 117–122.

WU, H., DING, A. A. and DE GRUTTOLA, V. (1998). Estimation of HIV dynamic parameters. *Statist. Med.* **17** 2463–2485.

WU, H. and DING, A. A. (1999). Population HIV-1 dynamics in vivo: Applicable models and inferential tools for virological data from AIDS clinical trials. *Biometrics* **55** 410–418.

WU, H., HUANG, Y. ET AL. (2005). Modeling antiretroviral response: Effects of drug potency, pharmacokinetics, adherence and drug resistance. *Journal of Acquired Immune Deficiency Syndromes* **39** 272–283.

WU, L. (2002). A joint model for nonlinear mixed-effects models with censoring and covariates measured with error, with application to AIDS studies. *J. Amer. Statist. Assoc.* **97** 955–964. MR1951254

ZHU, L. and CARLIN, B. P. (2000). Comparing hierarchical models for spatio-temporally misaligned data using the deviance information criterion. *Stat. Med.* **19** 2265–2278.

Y. HUANG
DEPARTMENT OF EPIDEMIOLOGY
AND BIOSTATISTICS
COLLEGE OF PUBLIC HEALTH, MDC 56
UNIVERSITY OF SOUTH FLORIDA
TAMPA, FLORIDA 33612
USA
E-MAIL: yhuang@health.usf.edu

H. WU
J. HOLDEN-WILTSE
DEPARTMENT OF BIOSTATISTICS
AND COMPUTATIONAL BIOLOGY
SCHOOL OF MEDICINE AND DENTISTRY
UNIVERSITY OF ROCHESTER
ROCHESTER, NEW YORK 14642
USA
E-MAIL: hwu@bst.rochester.edu
Jeanne_Wiltse@URMC.Rochester.edu

E. P. ACOSTA
BIRMINGHAM SCHOOL OF MEDICINE
UNIVERSITY OF ALABAMA
DIVISION OF CLINICAL PHARMACOLOGY
1530 3RD AVENUE SOUTH
BIRMINGHAM, ALABAMA 35294
USA
E-MAIL: Edward.Acosta@ccc.uab.edu